

$\pi g_{9/2} \otimes \nu g_{9/2}$  multiplet: Nuclear structure of  $^{82}\text{Y}$ G. García-Bermúdez,\* H. Somacal, M. A. Cardona, A. Filevich,\*  
E. Achterberg, and L. Szybisz\**Laboratorio TANDAR, Departamento de Física, Comisión Nacional de Energía Atómica,  
Avenida del Libertador 8250, 1429 Buenos Aires, Argentina*

(Received 31 May 1994)

The level scheme of  $^{82}\text{Y}$  is investigated via the  $^{58}\text{Ni}(^{27}\text{Al}, 2pn)$  reaction at a beam energy from 75 to 105 MeV. Excitation functions and neutron- $\gamma$  coincidences were performed in order to obtain the isotopic identification of the measured  $\gamma$  rays. From the angular distribution,  $\gamma$ - $\gamma$ , and delayed coincidence data a decay scheme was constructed. It exhibits a sequence of levels with probable spin values ranging up to  $I^\pi = (17^+)$ , two of them being isomeric states. In particular, the nuclear structure below the  $I^\pi = (9^+)$  is analyzed. The interpretation of these states in terms of the  $\pi g_{9/2} \otimes \nu g_{9/2}$  multiplet is discussed.

PACS number(s): 21.10.-k, 23.20.-g, 27.50.+e

## I. INTRODUCTION

Most of the experimental information available in the intermediate mass region around  $A \approx 80$  has been collected by investigating the nuclear structure of even-even and odd-even nuclei. The analysis of such data clearly established the “softness” of the core nuclei adopted for their theoretical interpretation. This feature is mainly indicated by a rapid change of nuclear properties as a function of the mass number  $A$  (for a comprehensive discussion of this subject see, e.g., Nazarewicz *et al.* [1]).

During the last years the odd-odd nuclei started to attract the attention of several experimental groups, hence, more information about this kind of system became available. These investigations give the opportunity to study the residual proton-neutron interaction. In particular, there are very interesting situations where both an odd proton and an odd neutron occupy the same shell. One might thus obtain information about their interaction as well as about the polarization effect of the odd particles on the soft core.

Continuing with the systematic investigation of doubly-odd nuclei in this mass zone we have undertaken the study of  $^{82}\text{Y}$ , for which almost nothing was known when our experimental work started. At that time, the scarce data on  $^{82}\text{Y}$  were restricted [2] to the parity and half-life of the ground state,  $I^\pi = 1^+$  and 9.5 s, and no excited states were known. For this reason an important part of the experiment was devoted to the isotopic identification of the measured  $\gamma$  radiation. A preliminary level scheme for  $^{82}\text{Y}$  obtained from our data has been already published elsewhere [3]. When our work was almost finished the research of two other groups on this nuclide

came to our attention. Womble *et al.* [4] determined levels up to  $I^\pi = 21^+$  and, on the other hand, a preliminary report of Mukai *et al.* [5] extended the spectrum to even higher angular momenta using a large array of detectors. We shall compare our results with the data of [4,5] in the final sections.

The paper is organized in the following way. The experimental setup and the procedures employed for the measurements, together with the results, are given in Sec. II. The proposed level scheme is presented in Sec. III. Finally, Sec. IV is devoted to a discussion and conclusions.

## II. EXPERIMENTAL PROCEDURE AND RESULTS

Several experiments were carried out by using the available beams provided by the Buenos Aires TANDAR accelerator to populate levels of  $^{82}\text{Y}$ . The isotopic identification of the numerous  $\gamma$  rays was performed by analyzing excitation functions of several reactions and neutron- $\gamma$  coincidence measurements. In practice, almost the same setup devised to investigate the  $^{89}\text{Mo}$  nuclide [6] was utilized in the present work. After selecting the most appropriate reaction and beam energy, the decay scheme of  $^{82}\text{Y}$  was primarily determined by means of  $\gamma$ - $\gamma$  coincidence experiments. The half-life of the isomeric state was measured using the delayed coincidence method with a pulsed beam.

## A. Isotopic identification

As mentioned above, two different sorts of experiments, namely excitation functions and neutron- $\gamma$  coincidences, were performed in order to obtain the isotopic

\*Also at the Carrera del Investigador Científico of the Consejo Nacional de Investigaciones Científicas y Técnicas, Argentina.

identification of the measured  $\gamma$  rays. For the neutron- $\gamma$  coincidence, the reaction  $^{58}\text{Ni}(^{28}\text{Si}, 3pn)$  was used at a beam energy of 110 MeV. The neutrons were detected with a 127 mm diameter by 127 mm long cylinder filled with NE213 liquid scintillator. This detector was positioned at 10 cm from the target and at  $0^\circ$  relative to the beam direction, and to decrease the number of detected  $\gamma$  rays it was covered with a 4 cm thick lead shield. The standard pulse shape discrimination technique was used to separate neutrons from  $\gamma$  rays. A HPGe detector of 40% efficiency located at  $135^\circ$  measured the  $\gamma$ -ray spectrum in coincidence with the neutron signal. The analysis determined that several strong  $\gamma$  rays, such as the 109, 211, and 244 keV lines, are in coincidence with neutrons and, hence, they belong to the decay of excited levels of the  $3pn$  channel leading to  $^{82}\text{Y}$ . Other reactions were disregarded. For instance, the channel involving the evaporation of  $\alpha 2pn$  and  $\alpha 3pn$  leads to known nuclides like  $^{79}\text{Sr}$  and  $^{78}\text{Rb}$ , respectively. Furthermore, reactions with more than one evaporated neutron are highly hindered in this mass zone as the evaporation code PACE4 predicts.

For the excitation function experiment,  $\gamma$ -ray singles spectra were measured using a Compton-suppressed HPGe detector of 30% efficiency placed at  $90^\circ$  with respect to the beam direction. The intensities of the  $\gamma$  rays were determined as a function of beam energy in steps of 5 MeV for the following reactions: (a)  $^{60}\text{Ni}(^{28}\text{Si}, \alpha pn)$  from 100 to 130 MeV; (b)  $^{58}\text{Ni}(^{28}\text{Si}, 3pn)$  from 95 to 120 MeV; and (c)  $^{58}\text{Ni}(^{27}\text{Al}, 2pn)$  from 75 to 105 MeV. Figure 1 shows the excitation function of several  $\gamma$  rays produced by reactions involving three or four outgoing particles, namely the  $2pn$  and  $3pn$  reaction channels. The shape and maxima of these curves are compatible with the behavior predicted by the evaporation code PACE4 for  $\gamma$  rays deexciting levels in  $^{82}\text{Y}$ . All these experiments support the results obtained with the previous neutron coincidence measurement and select the aluminium beam at 90 MeV as the best beam-energy combination to populate levels of the  $^{82}\text{Y}$  nucleus.

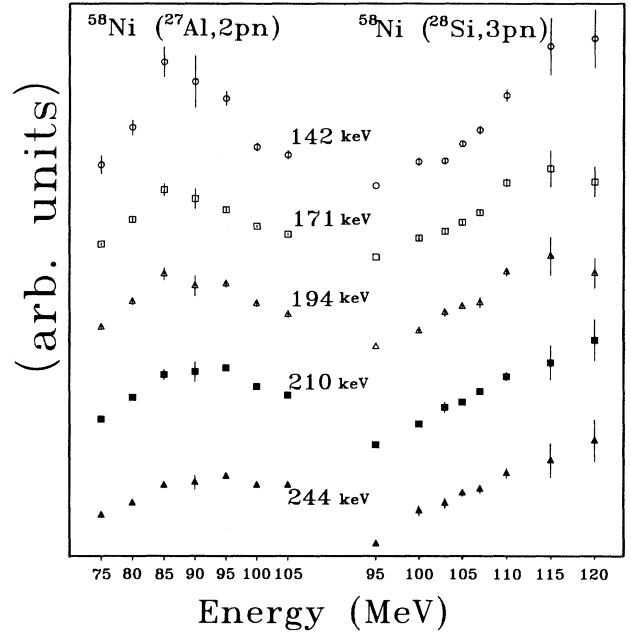


FIG. 1. Excitation function of several  $\gamma$  rays of  $^{82}\text{Y}$  produced by different reactions involving two and three outgoing particles, namely  $2pn$  and  $3pn$ . The  $2pn$  channel shows a maximum of intensity at about 85 – 90 MeV and the other,  $3pn$ , peaks at 115 – 120 MeV.

### B. $\gamma$ - $\gamma$ coincidence experiment

The  $\gamma$ - $\gamma$  coincidence experiment was performed using two Compton-suppressed HPGe detectors of 30% efficiency placed at  $90^\circ$  with respect to the beam direction. The used reaction was  $^{58}\text{Ni}(^{27}\text{Al}, 2pn)$  at 90 MeV beam energy, and the target consisted of a  $1.5 \text{ mg/cm}^2$  foil of  $^{58}\text{Ni}$  enriched to 99.9%, which was backed with a  $5 \text{ mg/cm}^2$  foil of natural bismuth in order to stop the re-

TABLE I. Energies, intensities, and angular distribution coefficients of  $\gamma$  rays assigned to  $^{82}\text{Y}$ . The error in the last digit is given in parentheses.

$E_\gamma$ (keV)	$I_\gamma^a$	$A_{22}$	$E_\gamma$ (keV)	$I_\gamma^a$	$A_{22}$
63.5(3)	200 <sup>b</sup>		250.2(2)	220	
64.1(3)	250 <sup>b</sup>		313.7(2)	450	
65.6(3)	180		337.2(2)	340	
87.5(3)	780		370.5(2)	270	-0.4(1)
88.9(3)	200		395.7(2)	380	-0.6(1)
106.4(4)	720 <sup>b</sup>		443.1(3)	145	
107.9(4)	60 <sup>b</sup>		812.5(3)	190	
109.2(2)	230		837.7(2)	500	
142.3(2)	1000		1010.6(5)	290	
171.4(2)	490		1060.0(5)	150	
194.8(2)	490		1171.5(5)	250	
211.2(2)	480	-0.43(4)	1313.1(1)	170	
244.0(2)	560	0.44(4)			

<sup>a</sup>The errors are 5% for the strongest peak and 30% for the weaker ones.

<sup>b</sup>The intensities are estimated from the coincidence results. The errors are 30%.

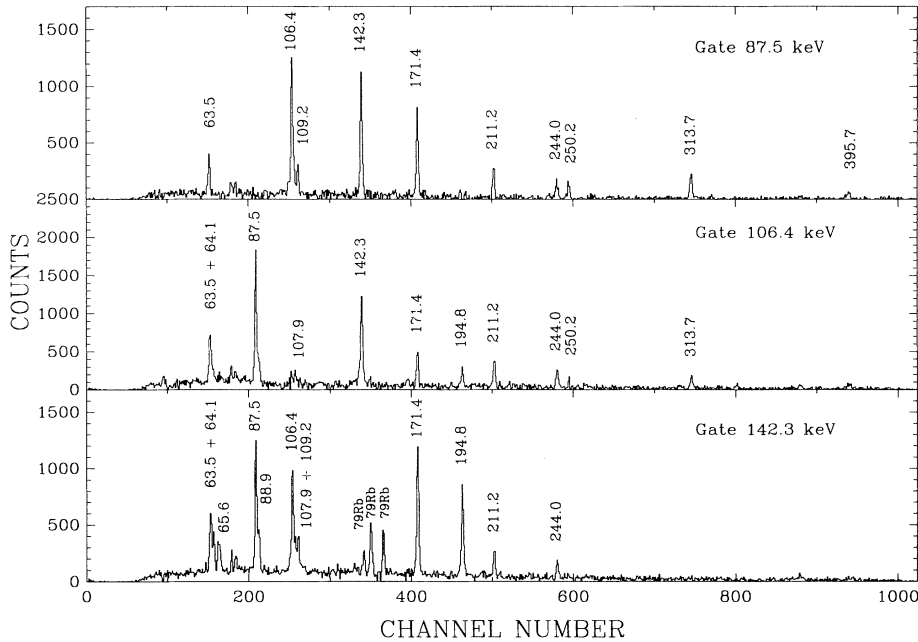


FIG. 2. Coincidence spectra with gates set on the 87.5, 106.4, and 142.3 keV  $\gamma$  rays. These transitions populate levels below an isomeric state of 140 ns half-life. The figure also shows the prompt 211.2 and 244.0 keV transitions originated due to the 100 ns time windows used in the coincidence experiment.

coiling nuclei. Several gated spectra are shown in Figs. 2 and 3. From all these experiments, the  $\gamma$  rays listed in Table I were assigned to the decay of excited states in  $^{82}\text{Y}$ . A preliminary level scheme based on these data has been already published elsewhere [3]. The revised and completed final version is shown in Fig. 4. As can be observed the decay scheme of  $^{82}\text{Y}$  shows: (a) many low-energy  $\gamma$  rays grouped at low energy and (b) a more regular level energy pattern developed toward higher angular momentum. In addition, the coincidence experiment identified a

reduction in the coincidence rate between certain  $\gamma$  rays, indicative of the existence of an isomeric state.

### C. Delayed coincidences

In order to determine the existence of isomeric states and to measure their half-lives a delayed coincidence experiment was performed. In this experiment we used

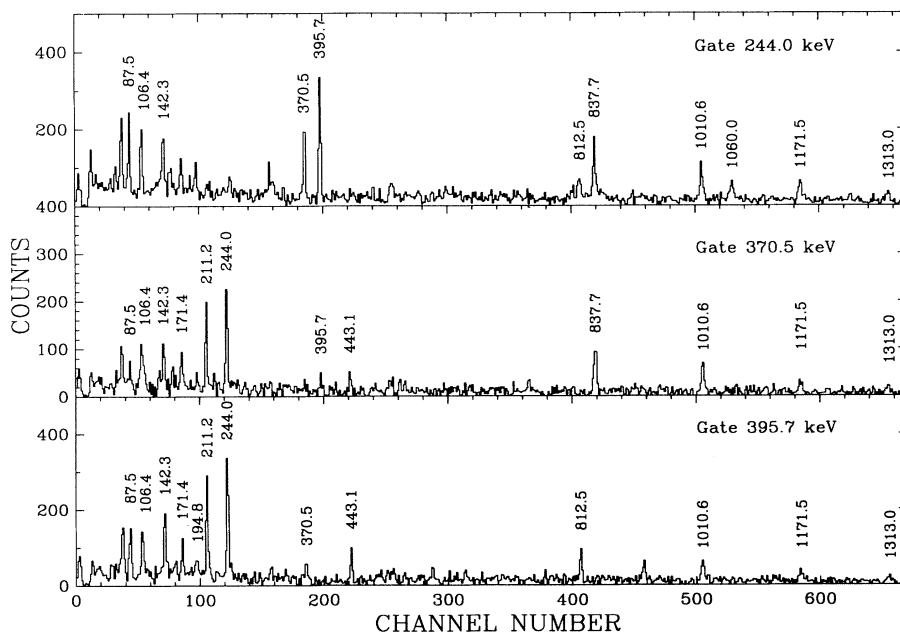


FIG. 3. Coincidence spectra with gates set on the 244.0, 370.5, and 395.7 keV  $\gamma$  rays. These transitions populate prompt levels above an isomeric state of 140 ns half-life. Some coincidence with transitions below the isomeric state, such as the 87.5, 106.4 keV, etc., lines, are due to the 100 ns time windows used in the coincidence experiment.

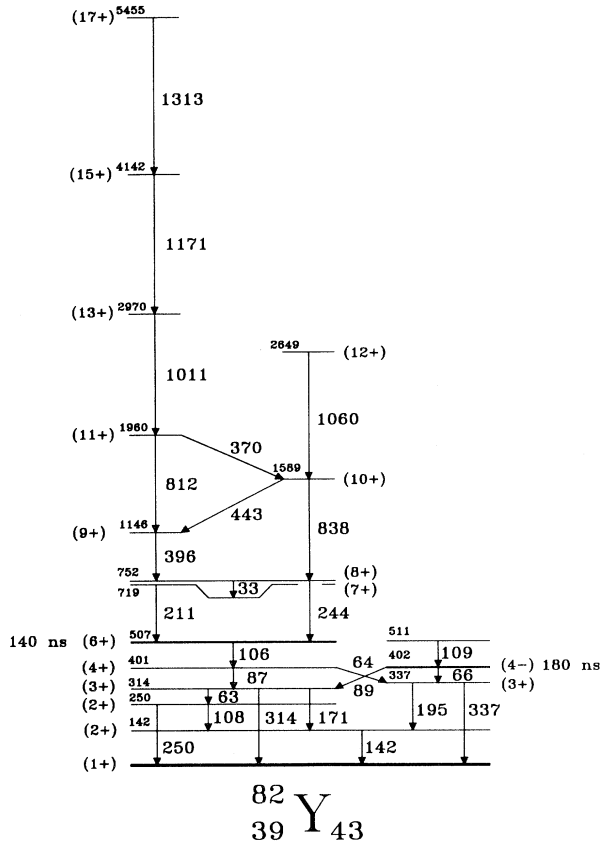


FIG. 4. Level scheme for  $^{82}\text{Y}$  derived in the present work. Two isomeric states of 140 and 180 ns half-lives were determined. The change in nuclear structure at about  $I^\pi = 8^+$  is apparent.

a chopped aluminium beam reacting with a nickel target. The time structure of the beam consisted of a 20 ns wide beam pulse followed by a silent period of 250 ns. The time-to-amplitude converter (TAC) was started by the  $\gamma$  rays detected by one of the HPGe detectors and stopped by an electronic signal time correlated with the beam burst. Therefore, the time window covered by this measurement was extended from about 50 up to 300 ns. Figure 5 shows prompt and delayed spectra in which energy labeled peaks belong to the decay of  $^{82}\text{Y}$ . There are several  $\gamma$  rays, such as the 211.2, 244.0, 370.5, and 395.7 keV transitions, that are not seen in the delayed spectrum which indicate that they are deexciting levels above the isomeric states. On the other hand, the energy and the intensity of weak  $\gamma$  rays are measured in better conditions in the decay spectrum, due to the considerable background reduction. From the data analysis, two groups of  $\gamma$  rays with a different half-life were found in the time range covered by this experiment. Figure 6 shows two representative  $\gamma$  rays of each group; these are the 87.5 – 106.4 keV and the 88.9 – 65.6 keV pairs which decay with half-lives of 140(20) and 180(90) ns, respectively. These two isomeric states decay, as shown in Fig. 4, through several low-energy transitions. Two of them, namely the 64 and 89 keV lines, connect levels populated by the two different isomers. The subsequent  $\gamma$  rays which are populated by both isomers do not present well-defined half-lives.

### III. THE LEVEL SCHEME

The level scheme was constructed on the basis of the  $\gamma$ - $\gamma$  coincidence experimental data in conjunction with

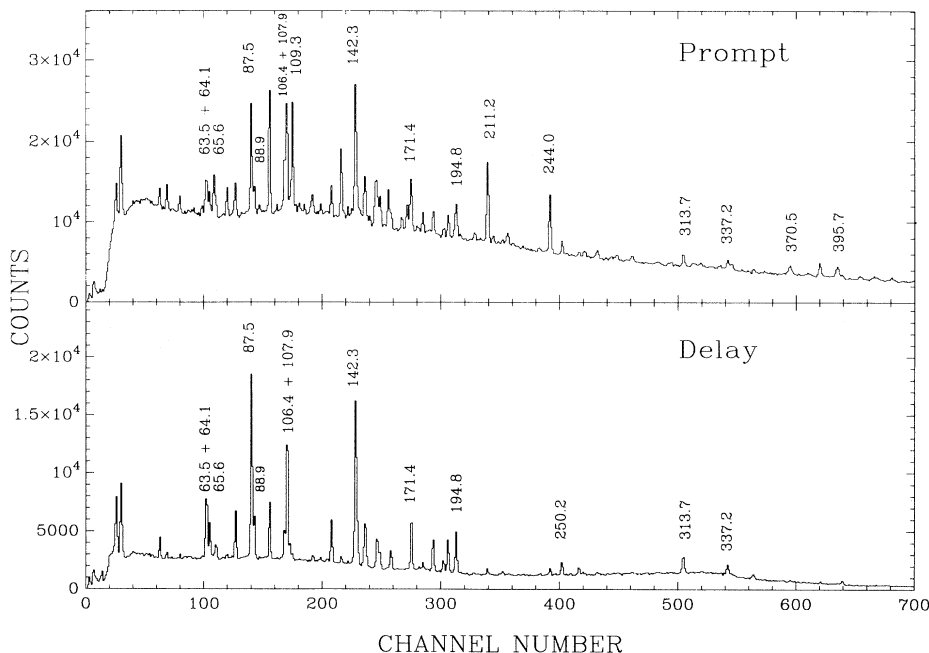


FIG. 5. This figure shows the prompt and delayed spectra where the peaks labeled by energy belong to the decay of  $^{82}\text{Y}$ . Notice that several  $\gamma$  rays measured in the prompt spectrum, such as the 211.2, 244.0, 370.5, and 395.7 keV lines, are not present in the delayed spectrum which indicates that they are deexciting levels above the isomeric state.

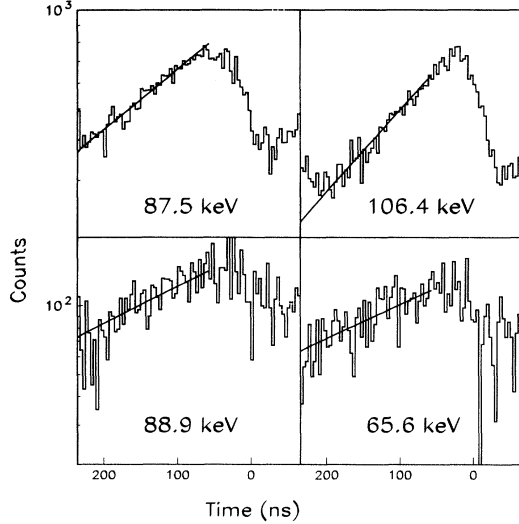


FIG. 6. Decay spectra of the 87.5 – 106.4 keV and 88.9 – 65.6 keV pairs of  $\gamma$  rays, whose half-lives are 140(20) and 180(90) ns, respectively.

$\gamma$ -intensity balances and energy combinations. The connection between the prompt and the delayed part of the decay scheme was performed by time coincidence and intensity balance. The half-life of the isomeric states is comparable to the time window used in the coincidence device ( $\approx 100$  ns); therefore it is possible to observe the coincidence between  $\gamma$  rays feeding and deexciting the isomeric state with a natural loss in the coincidence rate.

The proposed decay scheme for  $^{82}\text{Y}$  shown in Fig. 4 presents many characteristics in common with other nuclei in the  $A \approx 80$  mass region. It is well known that the microscopic structure of these nuclei is primarily determined by the filling of the “normal”  $p_{1/2}$ ,  $f_{5/2}$ , and  $p_{3/2}$  shells and the “intruder”  $g_{9/2}$  shell. The coupling of two particles in these orbits and their interaction with the core nucleus produce a wealth of different nuclear structure effects, some of them responsible for the appearance of isomerism. The numerous isomeric states found in this mass zone have in many cases lifetimes long enough to interrupt the time coincidence and, hence, to increase greatly the difficulty of the isotopic identification of the  $\gamma$  rays. Another feature observed in the case of doubly-odd nuclei is the population of the  $\pi g_{9/2} \otimes \nu g_{9/2}$  multiplet near the ground state. This multiplet reaches approximately the maximum angular momentum for the two quasiparticle system, namely  $I^\pi = 8^+ \text{ or } 9^+$ , and from there on a collective band is developed. The decay of  $^{82}\text{Y}$  clearly exhibits this characteristic. From the ground state up to 507 keV energy, the decay presents many low-energy  $\gamma$  rays and an erratic decay pattern, typically due to the coupling of quasiparticles.

Above the isomeric states, at an energy higher than 752 keV, the regular increase in level energy and the presence of crossover transitions are a clear signature of a collective band. The existence of isomeric states with half-lives of the order of 200 ns prevents us from using

the standard angular distributions measurement in order to obtain the spins of the levels.

On the other hand, the presence of such isomers allows an accurate determination of the  $\gamma$ -ray intensity balance for levels below them due to the absence of interference effects caused by side feeding. These measurements and the low  $\gamma$ -ray energies with total intensity (i.e.,  $\gamma$  intensity plus internal conversion), which are very sensitive to the multipole order of the transitions, provided the basic tools for the following spin assignment. The general idea is to start assuming a spin  $I$  for the isomeric state at 507 keV and, subsequently, to go down along the decay scheme assigning spins according to a well-accepted criterion until one reaches the ground state with known spin  $I^\pi = 1^+$ . In the following paragraphs it is shown that using this procedure it is possible to obtain the spin of all the low-lying levels in a consistent way.

Due to the long half-life of the 507 keV level a quadrupole character for the deexciting 106 keV transition is favored. Then we propose a level at 401 keV with spin  $I - 2$ , which decays through two low-energy  $\gamma$  rays of 64 and 87 keV. The absence of a long half-life suggests a dipole character for both transitions. Therefore the suggested spin for both the 314 and 337 keV levels is  $I - 3$ .

The measured branching ratios for each  $\gamma$ -ray deexciting levels below the isomers are listed in Table II together with the corresponding theoretical values. The reported theoretical ratios of  $\gamma$ -ray strengths were calculated from the tabulated Weisskopf values and corrected by considering the systematics in this mass zone. This correction consists of an enhancement factor of 10 for the quadrupole transitions and a hindrance factor of 0.01 for the magnetic ones, these values having been obtained from the extensive review study for the  $A = 45 - 90$  mass region performed by Endt [7].

Continuing with the analysis of the level at 314 keV, it decays among several transitions through a low-energy 63 keV  $\gamma$  ray. The absence of a long half-life suggests a dipole character and thus a spin  $I - 4$  for the 250 keV level fed by the 63 keV transition. The branching ratio of the 314 and 171 keV transitions which populate the 142 keV level and the ground state, respectively, shown in Table II are consistent with a quadrupole 314 keV and a dipole 171 keV transition. Then we suggest  $I - 4$  and  $I - 5$  as the spins of the 142 keV level and the ground state, respectively. The same argument may be applied to the decay of the  $I - 3$  level at 337 keV which feeds the same levels. In this case the branching ratio for the 337 and 195 keV transitions (Table II) is also in agreement with a quadrupole to dipole ratio. In addition, the decay of the 250 keV level of spin  $I - 4$  also populates the 142 keV level and the ground state; in this case the measured branching ratio of the 108 and 250 keV transitions is consistent with a dipole to dipole ratio (Table II).

From all the previous arguments it is possible to suggest that the spin of the ground state is  $I - 5$ , and no parity change is necessary to be assumed in any step of the spin assignment procedure. Therefore, from the known spin and parity  $I^\pi = 1^+$  of the ground state it turns out that  $I^\pi = 6^+$  is the most probable assignment

TABLE II. The reported experimental branching ratios,  $I_r$  (measured), for low-energy levels  $E_{\text{level}}$  assigned to  $^{82}\text{Y}$ , which deexcite through two  $\gamma$  rays indicated by  $(\gamma_1, \gamma_2)$ . These ratios include the internal conversion correction for the different multipolarities [i.e.,  $(E_2, M_1)$ ,  $(M_1, M_1)$ ,  $(E_1, E_1)$ , and  $(E_2, E_2)$ ]. The theoretical ratios,  $I_r$  (calculated), were obtained from the tabulated Weisskopf values corrected by considering the systematics in this mass zone.

$E_{\text{level}}$ (keV)	$(\gamma_1, \gamma_2)$ (keV)	$I_r$ (measured) <sup>a</sup>		$I_r$ (calculated) <sup>a</sup>	
		$E_2, M_1$	$M_1, M_1$	$E_2, M_1$	$M_1, M_1$
337	337, 195	0.68		0.52	
314	314, 171	0.89		0.54	
	171, 63	1.50	1.53	0.50	19.6
401	64, 87		0.41		0.39
250	108, 250	0.48	0.31	0.001	0.08
402	66, 89	$E_1, E_1$		$E_1, E_1$	
		1.07		0.40	0.03

<sup>a</sup> $I_r = I(\gamma_1)/I(\gamma_2)$ . The estimated errors are 20%.

for the isomeric state at 507 keV, from which this analysis started.

The isomeric level at 402 keV decays through two low-energy transitions of 89 and 66 keV, which exhibit a branching ratio suggesting that both transitions are of dipole character. The existence of a state with a long half-life deexcited by low-energy dipole  $\gamma$  rays is consistent with transitions of electric character and therefore involving a change of parity. Thus  $I^\pi = 4^-$  is assigned to the 402 keV level. This assignment also explains the absence of any transition connecting this state with the higher-lying isomer  $I^\pi = 6^+$  at 507 keV.

The measured angular distributions quoted in Table I indicate that the transitions of 211 and 244 keV, located just above the isomeric  $6^+$  state, are of dipole and quadrupole character, respectively. Hence  $7^+$  and  $8^+$  are the spins assigned for the 719 and 752 keV states. On top of these states a regular increase of level energy and numerous crossover transitions, characteristic of a collective band, suggest the spin assignments shown in Fig. 4. The angular distributions for the 396 and 370 keV transitions indicate a dipole character giving additional support to the previous assignment. In a recent work, Womble *et al.* [4] have used an array of  $\gamma$ -ray detectors in order to determine the decay scheme of  $^{82}\text{Y}$ . They also measured directional correlation ratios (DCO), picosecond lifetimes via the Doppler-shift attenuation method, and delayed coincidences. Their decay scheme and the present one are in good agreement. Since the position in the decay scheme for the unobserved 33 keV transition feeding either the 507 or the 719 keV level is uncertain in the present work, it was placed according to the assignment proposed by Womble *et al.* [4].

#### IV. DISCUSSION

The nuclear structure in the vicinity of the  $A \approx 80-90$  mass region cannot be described by using a unique nuclear shape due to the “softness” of the core presented by these nuclei. The rapid changes of the shape with particle number, the rotational frequency, the polarization

effect of the odd particle, and even different shapes in the same nucleus are well-known features. All these phenomena indicate that we have to be cautious in making use of the concept of shape.

Let us begin a brief review of some nuclear properties in this mass region looking at data for doubly-even nuclei lying in the proximity of  $^{82}\text{Y}$ . Figure 7 shows the evolution as a function of the neutron number of two important parameters for the structure of Sr and Zr isotopes, which are sensible to the nuclear shape. These quantities were collected by Hüttmeier *et al.* [8] being the  $B(E2)$  values of the first  $2^+$  states and the energy ratios be-

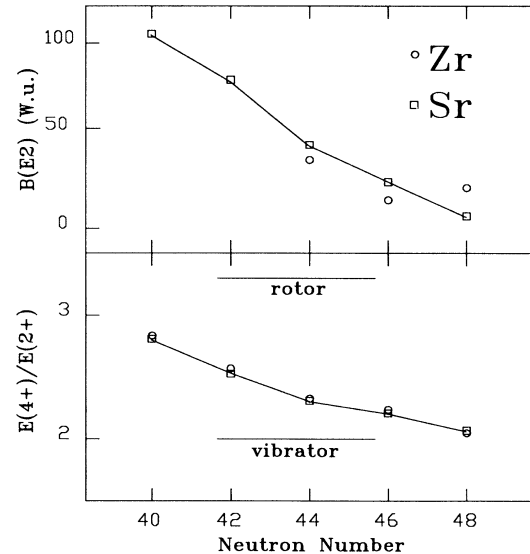


FIG. 7. Energy ratios  $E(4^+)/E(2^+)$  and  $B(E2)$  values as a function of the neutron number  $N$  for doubly even Sr and Zr isotopes. This energy ratio has a theoretical value of 2 for a perfect vibrator and of 3.33 for a rigid rotor; both these results are plotted in the figure in order to set a reference frame. The core of the  $^{82}\text{Y}$  nucleus, which lies in the vicinity of  $N = 42-44$ , would have near the ground state an intermediate deformation close to the spherical minimum.

tween the  $4^+$  and  $2^+$  states, i.e.,  $E(4^+)/E(2^+)$ . This ratio has a theoretical value of 2 for a perfect vibrator and amounts to 3.33 for a rigid rotor. As can be observed in the figure, the energy ratio parameter presents a smooth behavior going from a vibrator at  $N = 48$  to almost a rotor at  $N = 40$ . The  $B(E2)$  values also follow this trend going from few single-particle units at  $N = 48$  up to a collective value of about 100 single-particle units for  $N = 40$ . This smooth change between spherical and deformed shape is characteristic of finite many-body systems. These two parameters are sensible to the nuclear shape near the ground state. Hence the core of the  $^{82}\text{Y}$  nucleus, which lies in the vicinity of  $N = 42 - 44$ , would have an intermediate deformation close to the spherical minimum.

A more detailed picture of the shape as a function of angular momentum may be obtained by analyzing the high-spin data of the neighboring even-even and odd-even nuclides, namely  $^{82}\text{Sr}$  and  $^{83}\text{Zr}$ . The cranking model analysis of bands of  $^{82}\text{Sr}$  performed by Baktash *et al.* [9] reveal a rich variety of nuclear deformations which exhibit prolate, oblate, and triaxial shapes. Moreover, it may be seen in Fig. 2 of [9] that the deformation of the ground-state band increases from spherical, at spin zero, to a large deformation value of  $\beta_2 = 0.34$  at spin  $I = 6$ . Different theoretical models [1,10], which describe this mass zone predicting the appearance of prolate and oblate shapes, agree that for  $N = 44$  the spherical shape is favored for the ground state. The interplay of the different shapes can be qualitatively described by taking into account the different energy gaps which appear in the deformed shell model at neutron number 38 and 40. These energy gaps can stabilize spherical as well as other deformed shapes.

Figure 8 shows for several doubly-even neighbors of  $^{82}\text{Y}$  a systematics of available data [9,11–15] for the kinematic moment of inertia

$$\mathcal{J}^{(1)} = I/(dE/dI) \quad (1)$$

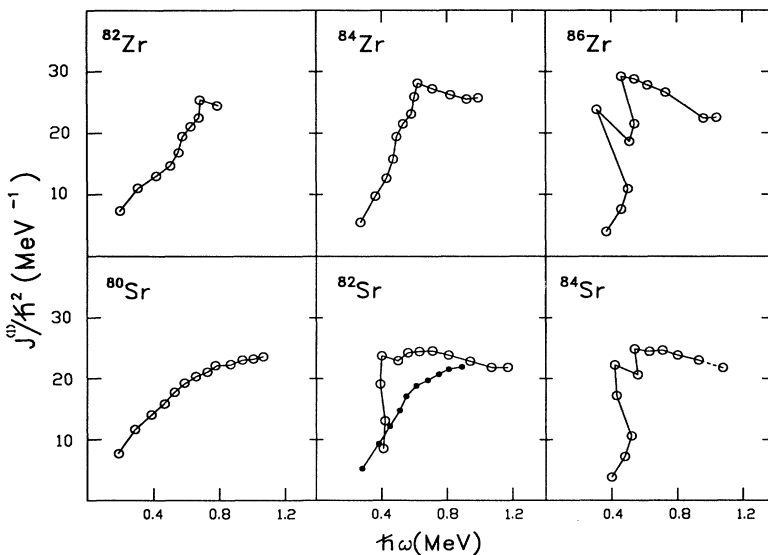


FIG. 8. Kinematic moment of inertia as a function of rotational frequency for the “yrast” positive-parity band of doubly even Sr and Zr isotopes. The data of  $^{82,84,86}\text{Zr}$  are from Mitarai *et al.* [11], Price *et al.* [12], and Chowdhury *et al.* [13], respectively. The data of  $^{80,82,84}\text{Sr}$  are from Davie *et al.* [14], Baktash *et al.* [9], and García-Bermúdez *et al.* [15], respectively. In particular, for the  $^{82}\text{Sr}$  nucleus the figure shows the ground-state band (filled circles) and the positive-parity band with bandhead at 1175.6 keV energy (open circles). The figures show a similar sudden rise of the kinematic moment of inertia followed by a sort of saturation.

as a function of the rotational frequency  $\hbar\omega$ , which is also related to the derivative of the energy since

$$\omega = dE/dI. \quad (2)$$

From the observation of Fig. 8 it turns out that there are some common features. For instance, all the data show a similar sudden rise of the kinematic moment of inertia followed by a sort of saturation. The first part could be related to a “spherical” structure since the constancy of the  $\gamma$ -ray energies with spin entails a constant frequency, which is a characteristic of a vibrational structure. On the other hand, a kinematic moment of inertia independent of the frequency is characteristic of a rigid-rotor behavior. All these nuclei present a common value of the kinematic moment of inertia at high frequencies, which is approximately equal to the rigid moment of inertia. A more detailed discussion of these effects may be found in the study of  $^{82}\text{Sr}$  [9] and in a recent survey of Tabor [16] who analyzed in detail the convergence of the kinematic moments of inertia at frequencies above  $\hbar\omega = 0.6$  MeV. The latter survey indicates interesting trends but also suggests a need of much more experimental work to describe in greater detail the nuclear structure in this spin region.

After this summary of properties of some neighbors of  $^{82}\text{Y}$ , we can conclude that they exhibit features of very “soft” nuclei. Let us now discuss with more detail the measured decay scheme of  $^{82}\text{Y}$  shown in Fig. 4. Since at the level with spin  $I^\pi = 9^+$  a change of nuclear structure is apparent, for the sake of clarity, the following discussion is divided into two subsections. One of them deals with the spectrum above the  $I^\pi = 9^+$  state and the other is devoted to levels below it.

#### A. The structure above the $9^+$ state

It may be seen that on top of the  $I^\pi = 9^+$  level a normal collective band is developed. Figure 9 shows the

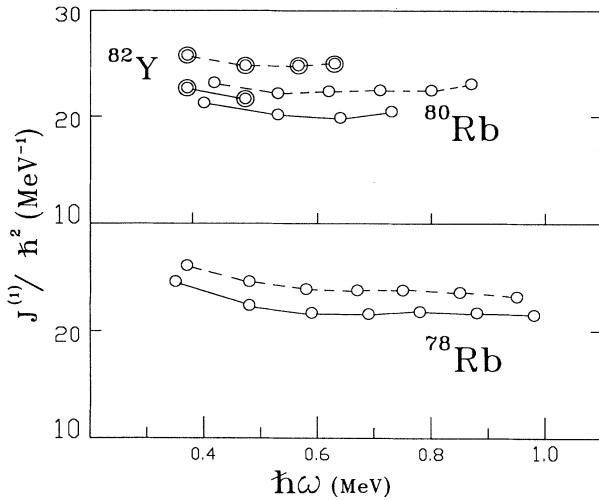


FIG. 9. Kinematic moment of inertia as a function of rotational frequency for  $^{82}\text{Y}$  above the  $I^\pi = 9^+$  state compared with results for  $^{78}\text{Rb}$  [17] and  $^{80}\text{Rb}$  [18,19]. All these bands present an almost constant kinematic moment of inertia and for different signatures exhibit a similar splitting of their values (solid and dashed lines) for a large part of the frequency range. The observed similarities strongly support a common underlying structure.

kinematic moment of inertia  $\mathcal{J}^{(1)}$  for this band in comparison with similar band structures found in  $^{78}\text{Rb}$  [17] and  $^{80}\text{Rb}$  [18,19]. All these bands present an almost constant kinematic moment of inertia and for different signatures exhibit a similar splitting of their values for a large part of the frequency range. The observed similarities strongly support a common underlying structure

where both odd particles occupy the intruder  $g_{9/2}$  shell. A recent systematic study of this kind of band structure in Rb and Br isotopes [19] established that their decay schemes are divided into two regions at the  $8_1^+$  level: collective bands above this state and more irregular patterns of levels below it. The angular momentum at which this change occurs is correlated approximately with the highest angular momentum obtained from the intrinsic motion of two  $g_{9/2}$  particles in an odd-odd nucleus ( $I^\pi = 9^+$ ). In a recent work [4], the Woods-Saxon cranking model with a particle rotor has been applied to describe the positive-parity band of  $^{82}\text{Y}$ . The authors interpreted this band as having a triaxial shape with a moderate quadrupole deformation  $\beta_2 = 0.25$ .

**B. The structure below the  $9^+$  state**

Below the  $I^\pi = 9^+$  level the decay scheme presents an irregular pattern with two isomeric states and many low-energy transitions. It is well known that the microscopic structure of nuclei in the  $A \approx 80 - 90$  mass region is primarily determined by the filling of the normal odd-parity  $p_{3/2}$ ,  $f_{5/2}$ , and  $p_{1/2}$  shells and the intruder shell of even-parity  $g_{9/2}$ . Then in first-order approximation, without any residual interaction, the low-spin positive-parity states of  $^{82}\text{Y}$  up to spin  $9^+$  could be described by the  $\pi g_{9/2} \otimes \nu g_{9/2}$  structure, probably with an admixture of states where both particles are in the  $p_{1/2}$ ,  $f_{5/2}$ , and  $p_{3/2}$  orbitals which span over the spin region from  $1^+$  up to  $5^+$ .

In an attempt for correlating the known low-energy positive-parity levels of  $^{82}\text{Y}$  with other probable members of the  $\pi g_{9/2} \otimes \nu g_{9/2}$  multiplet, which enclose the spin region from  $0^+$  up to  $9^+$ , we show in Fig. 10 the

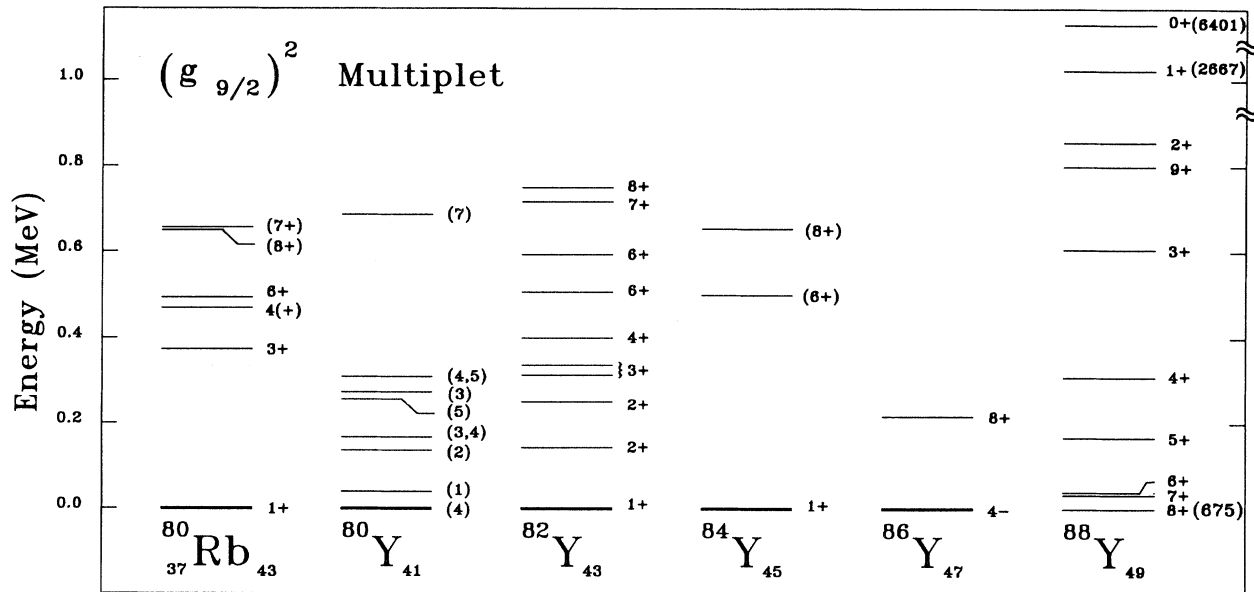


FIG. 10. Systematics of the low-energy positive-parity levels of several odd-odd Y isotopes and the  $^{80}\text{Rb}$  nucleus [18]. The data of  $^{80,84,86}\text{Y}$  are from Lister [20], Chattopadhyay *et al.* [21], Bucurescu *et al.* [22], and the  $^{88}\text{Y}$  levels obtained from the review work of Schiffer and True [23].

systematics of such levels for several odd-odd Y isotopes [20–23] and the  $^{80}\text{Rb}$  nuclide [18].

In particular, the level scheme of  $^{82}\text{Y}$  starts with a ground state of spin  $1^+$ , it exhibits several doublets, as the  $2^+$ ,  $3^+$ , and  $6^+$  ones, and the absence of a  $5^+$  state. Let us look first at the pair  $^{80}\text{Y}$ - $^{82}\text{Y}$ . It becomes apparent from Fig. 10 that even though the  $^{80}\text{Y}$  decay scheme is not well known it presents several levels with the same spin at approximately the same energy, compared with  $^{82}\text{Y}$ . Moreover, a better-known nucleus which is an isotope of  $^{82}\text{Y}$ , namely  $^{80}\text{Rb}$ , also presents a rather similar level scheme. This parallelism suggests a common underlying nuclear structure. Due to the proximity of both particle numbers to the semimagic numbers  $Z = 38$  and  $N = 40$  and the start of the filling of the  $g_{9/2}$  shell at particle number 40, one may suggest that the observed positive-parity states could be described as a particle excitation in the  $g_{9/2}$  shell.

Continuing with the discussion of Fig. 10 towards heavier nuclei, it shows that for  $^{84}\text{Y}$  and  $^{86}\text{Y}$  only few positive-parity levels have been reported. However, in the proximity of the closed shell  $N = 50$ , that is, for  $^{88}\text{Y}$ , a very well-known nuclear structure is available. The  $^{88}\text{Y}$  is so well determined because it can be populated by many different light charge reactions which are particularly suitable to measure the single-particle contents of nuclear levels. The partial level scheme of  $^{88}\text{Y}$ , shown in Fig. 10, belongs to the  $g_{9/2}$  multiplet which starts at an energy of 675 keV for the  $8^+$  state and extends up to the  $1^+$  and  $0^+$  levels at the high energies of 2.7 and 6.4 MeV, respectively. From the numerous experimental studies of the nuclear structure of  $^{88}\text{Y}$  and  $^{90}\text{Nb}$ , which present one hole in the  $N = 50$  closed shell, it was possible to determine the complete set of matrix elements for the particle-hole  $\pi g_{9/2} \otimes \nu g_{9/2}^{-1}$  multiplet. The review study of Schiffer and True [23] describes in great detail the experiments as well as the theoretical ideas utilized to obtain these matrix elements.

It is possible to relate the well-known particle-hole multiplet determined in  $^{88}\text{Y}$  with  $^{82}\text{Y}$  if one assumes that the odd particle lying in a spherical  $\nu g_{9/2}$  shell can approximately describe the nuclear structure of  $^{82}\text{Y}$ . The proximity of this nucleus to the  $N = 40$  and  $Z = 38$  subshells as well as the different models described earlier, which predict together with a variety of nuclear shapes a spherical one near the ground state, supports this assumption. The relation between the particle-particle multiplet in  $^{82}\text{Y}$  and the particle-hole one of  $^{88}\text{Y}$  is given by the so-called ‘‘Pandya transformation’’ [24]. This algebraic transformation, see, e.g., (1.2) of [23], may be written as

$$E_I^{(p-p)}(j_1 j_2) = - \sum_{I'} (2I' + 1) W(j_1 j_2 j_2 j_1; II') \times E_I^{(p-h)}(j_1 j_2), \quad (3)$$

where for a fixed spin  $I$  the quantities  $E_I^{(p-p)}(j_1 j_2)$  and  $E_I^{(p-h)}(j_1 j_2)$  are the matrix elements for the particle-particle and particle-hole configurations, respectively. The factors  $W(j_1 j_2 j_2 j_1; II')$  which transform one matrix element into the other are the Racah coefficients.

By applying this transformation to the particle-hole multiplet of  $^{88}\text{Y}$  and  $^{90}\text{Nb}$  normalized to the lowest  $8^+$  level, one gets the results shown in Fig. 11. The multiplet is split into two groups of levels with different parity  $(-1)^I$ . This is because two nonidentical particles as the proton and the neutron lying in a common shell can be separated, due to the isospin formalism, into two groups of states corresponding to total isospin  $T = 1$  and  $T = 0$ . The generalized Pauli principle, which includes the isospin coordinate, relates the  $T = 1$  and  $T = 0$  groups of states with the  $I = \text{even}$  and  $I = \text{odd}$  angular momentum, respectively.

Figure 11 shows the  $T = 1$  and  $T = 0$  groups of particle-particle states calculated from the known  $^{88}\text{Y}$  and  $^{90}\text{Nb}$  nuclei as a function of angular momentum. It is apparent that the energy of the levels for isospin  $T = 0$  exhibits an inverted U shape, while for the isospin  $T = 1$  it rises monotonously with spin. This behavior can be explained by taking into account that the nuclear

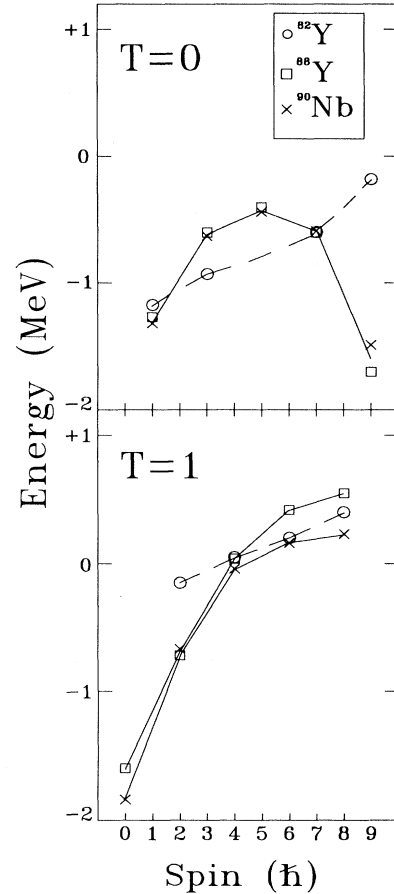


FIG. 11. Energy of the  $^{82}\text{Y}$  states as a function of angular momentum compared with the isospin  $T = 1$  and  $T = 0$  groups of the particle-particle multiplets calculated from data of the  $^{88}\text{Y}$  and  $^{90}\text{Nb}$  nuclei obtained from the review work of Schiffer and True [23]. The energy of the  $9^+$  level, being much higher than the predicted one, suggests that such a state might be better understood as part of the collective band rather than a part of the multiplet.

interaction is a short-ranged attractive force. For isospin  $T = 0$  the maximum overlap between the nucleon orbits, and therefore the maximum interaction, occurs when the angles of the orbits are approximately  $0^\circ$  or  $180^\circ$  which corresponds to  $I = 9^+$  and  $I = 1^+$ , respectively. On the other hand, for  $T = 1$  states and high-spin  $I$  it implies approximately spatial antisymmetry. Thus for the orbits that are coplanar the particles have to rotate out of phase and then the separation between them is large. For low spin the rotation is in the opposite direction, and therefore the overlap is large [23].

The  $^{82}\text{Y}$  decay scheme exhibits several pairs of levels with the same spin. For comparison only the average energy values for each spin are shown in Fig. 11. Furthermore, for normalization purposes the energies of the  $8^+$  and  $7^+$  levels of  $^{82}\text{Y}$  are set equal to the average energy of the  $8^+$  states and  $7^+$  of the  $^{88}\text{Y}$ - $^{90}\text{Nb}$  nuclei for  $T = 1$  and  $T = 0$ , respectively.

Let us first discuss the  $T = 1$  group of the  $^{82}\text{Y}$  states shown in Fig. 11. The matrix elements for the  $I = 4^+$ ,  $6^+$ , and  $8^+$  states of  $^{82}\text{Y}$  follow approximately the trend exhibited by the  $^{88}\text{Y}$ - $^{90}\text{Nb}$  multiplet, which shows for these spin values a small increase towards higher angular momentum. But the comparison for lower spins is less satisfactory, there is an important difference in the case of the  $2^+$  state, and the  $0^+$  state is absent.

In turn, in the case of the  $T = 0$  isospin multiplet the  $1^+$  matrix element coincides with that of the  $^{88}\text{Y}$ - $^{90}\text{Nb}$  pair of nuclides, the agreement for the  $3^+$  is worse and there is one member of the multiplet, namely the  $5^+$ , that is missing. However, since the predicted energy for the  $5^+$  state lies at higher energy than that of the  $7^+$  level the situation is not favorable to populate the former one. Furthermore, the measured  $9^+$  level, which lies at much higher energy than the predicted one for the member of the isospin multiplet, may be better understood as

a part of the collective band rather than a part of this multiplet. Hence, we suggest that the observed  $9^+$  state is the bandhead of the rotational band built up on top of it.

Concluding, there are several arguments that suggest that the low-energy positive-parity states of  $^{82}\text{Y}$  could be related to the  $\pi g_{9/2} \otimes \nu g_{9/2}$  multiplet. Certainly the experimental observation of only the energy and parity of the levels does not give such strong evidence to characterize properly the nuclear levels as that provided by light reaction measurements. These previous studies, in particular the one-particle transfer reaction, available for the  $^{88}\text{Y}$ - $^{90}\text{Nb}$  nuclei, are much more sensitive to the configurational purity of the states. Nevertheless the sum of several arguments suggests describing the low-energy levels as a result of two quasiparticles interacting with a weakly deformed core. Taking into account that the effective interaction of two nucleons in the  $g_{9/2}$  shell is already well known, then this information can be helpful to study the perturbation on the multiplet induced by weakly- or well-deformed shapes. More experimental effort in the study of the nuclear structure of  $^{80}\text{Y}$ ,  $^{80}\text{Rb}$ , as well as of  $^{82}\text{Y}$ , near the ground state, will greatly contribute to increase our knowledge about this effect.

*Note added.* We have learned that the final version of the preliminary results reported by J. Mukai *et al.* [5] have been already published in Nucl. Phys. **A568**, 202 (1994). Their data agree with ours and add some new bands and more levels at higher angular momentum.

## ACKNOWLEDGMENTS

The authors acknowledge partial support from the PID-CONICET and from the Fundación Antorchas (Argentina).

- 
- [1] W. Nazarewicz, J. Dudek, R. Bengtsson, T. Bengtsson, and I. Ragnarson, Nucl. Phys. **A435**, 397 (1985).
  - [2] H.-W. Müller, Nucl. Data Sheets **50**, 1 (1987).
  - [3] G. García-Bermúdez, H. Somacal, M. A. Cardona, A. Filevich, E. Achterberg, and L. Szybisz, in *International Symposium on Nuclear Physics of our Times*, edited by A. V. Ramayya (World Scientific, Singapore, 1993), p. 216.
  - [4] P. C. Womble, J. Döring, T. Glasmacher, J. W. Holcomb, G. D. Johns, T. D. Johnson, T. J. Petters, M. A. Riley, V. A. Wood, S. L. Tabor, and P. Semmes, Phys. Rev. C **47**, 2546 (1993).
  - [5] J. Mukai *et al.*, in *Progress Report 1991-1992*, Kyushu University, Hakozaki, Fukuoka, Japan, p. 78.
  - [6] G. García-Bermúdez, M. A. Cardona, R. V. Rivas, A. Filevich, E. Achterberg, and L. Szybisz, Phys. Rev. C **48**, 1623 (1993).
  - [7] P. M. Endt At. Data Nucl. Data Tables **23**, 547 (1979).
  - [8] U. J. Hüttmeier, C. J. Gross, D. M. Headly, E. F. Moore, S. L. Tabor, T. M. Cormier, P. M. Stwertka, and W. Nazarewicz, Phys. Rev. C **37**, 118 (1988).
  - [9] C. Baktash, G. García-Bermúdez, D. G. Sarantites, W. Nazarewicz, V. Abenante, J. R. Beene, H. C. Griffin, M. L. Halbert, D. C. Hensley, N. R. Johnson, I. Y. Lee, F. K. McGowan, M. A. Riley, D. W. Stracener, T. M. Semkow, and A. Virtanen, Phys. Lett. B **255**, 174 (1991).
  - [10] P. Bonche, H. Flocard, P. H. Heenen, S. J. Krieger, and M. S. Weiss, Nucl. Phys. **A443**, 39 (1985).
  - [11] S. Mitarai *et al.*, Z. Phys. A **344**, 405 (1993).
  - [12] H. G. Price, C. J. Lister, B. J. Varley, W. Gelletly, and J. W. Olness, Phys. Rev. Lett. **51**, 1843 (1983).
  - [13] P. Chowdhury *et al.*, Phys. Rev. Lett. **67**, 2950 (1991).
  - [14] R. F. Davie, D. Singlair, S. S. L. Ooi, N. Poffé, A. E. Smith, H. G. Price, C. J. Lister, B. J. Varley, and I. F. Wright, Nucl. Phys. **A463**, 683 (1987).
  - [15] G. García-Bermúdez *et al.*, Phys. Rev. C **49**, 3309 (1994).
  - [16] S. L. Tabor, Phys. Rev. C **45**, 242 (1992).
  - [17] W. Gelletly, Y. Abdelrahman, A. A. Chishti, J. L. Durell, J. Fitzgerald, C. J. Lister, J. H. McNeill, W. R. Phillips, and B. J. Varley, in *Nuclear Structure of the Zirconium Region*, edited by J. Eberth, R. A. Meyer, and K. Sistemich (Springer-Verlag, Berlin, 1988), p. 105.
  - [18] J. Döring, G. Winter, L. Funke, B. Cederwall, F. Liden, A. Johnson, A. Atac, J. Nyberg, G. Sletten, and M. Sug-

- awara, Phys. Rev. C **46**, 2127 (1992).
- [19] G. García-Bermúdez *et al.*, unpublished.
- [20] C. J. Lister, private communication.
- [21] S. Chattopadhyay, H. C. Jain, J. A. Sheikh, Y. K. Agarwal, and M. L. Jhingan, Phys. Rev. C **47**, 1 (1993).
- [22] D. Bucurescu, G. Constantinescu, D. Cutoiu, M. Ivascu, N. V. Zamfir, and A. Abdel Haliem, J. Phys. G **10**, 1189 (1984).
- [23] J. P. Schiffer and W. W. True, Rev. Mod. Phys. **48**, 191 (1976).
- [24] S. Pandya, Phys. Rev. **103**, 956 (1956).